

Control of Synapse Number by Glia

Erik M. Ullian,* Stephanie K. Sapperstein, Karen S. Christopherson, Ben A. Barres

Although astrocytes constitute nearly half of the cells in our brain, their function is a long-standing neurobiological mystery. Here we show by quantal analyses, FM1-43 imaging, immunostaining, and electron microscopy that few synapses form in the absence of glial cells and that the few synapses that do form are functionally immature. Astrocytes increase the number of mature, functional synapses on central nervous system (CNS) neurons by sevenfold and are required for synaptic maintenance *in vitro*. We also show that most synapses are generated concurrently with the development of glia *in vivo*. These data demonstrate a previously unknown function for glia in inducing and stabilizing CNS synapses, show that CNS synapse number can be profoundly regulated by nonneuronal signals, and raise the possibility that glia may actively participate in synaptic plasticity.

Astrocytes, which ensheath synapses throughout the CNS, are presently thought of as synaptic support cells, clearing ions and neurotransmitters from the synaptic cleft, but accumulating evidence suggests the possibility of more active roles as well (1–3). The role of glia at CNS synapses has been difficult to study because glial cells are present in CNS cultures and are often necessary for neuronal survival. In this study, we have taken advantage of recently developed methods to isolate a defined type of CNS neuron, retinal ganglion cells (RGCs), by immunopanning the cells to greater than 99.5% purity (4, 5) and then culturing them in a defined serum-free medium (5). Using these methods, we have previously shown that RGCs cultured in the presence of astrocyte-conditioned medium have 10 times higher levels of synaptic activity (6). This glial effect is not simply due to enhancement of RGC maturation, because RGCs cultured either in the presence or absence of glia are electrically excitable, develop comparable numbers of dendrites and axons, and have identical survival rates. In addition, RGCs cultured under both conditions synthesize, secrete, and respond to glutamate (6) and express nearly identical levels of mRNAs for a large battery of neurotransmitter receptors, voltage-dependent ion channels, and synaptic proteins, as assessed by gene chip analysis (7). In this study, we examine whether the increased synaptic activity in glia is due to an increase in the number of synapses or to the efficacy of synaptic transmission.

To address this question, we cultured pu-

rified RGCs in the presence or absence of astrocytes. RGCs were cultured for 1 week followed by the addition of astrocytes either in contact with RGCs or as a feeding layer for

RGCs (8). Similar results were obtained under both conditions. After 2 weeks in culture, we used whole-cell patch-clamp recording to measure the significant enhancement of spontaneous synaptic activity by astrocytes (Fig. 1, A and B) (9). In the absence of astroglia, little synaptic activity occurred even when RGCs were cultured with their tectal target cells (6). This difference in synaptic activity persisted even after a month in culture, indicating that it is not accounted for by a maturational delay. To examine whether glia regulate synaptic activity by enhancing postsynaptic responsiveness, we measured the response of RGCs to pulses of L-glutamate applied to the cell somas. Regardless of the presence of glia, RGCs responded with inward currents (Fig. 1C) that were blocked by glutamate receptor antagonists (10). The size of the postsynaptic response, however, was threefold larger in RGC neurons cultured with glia (Fig. 1D), consistent with the increased amplitude of spontaneous synaptic miniature events (miniature excitatory postsynaptic currents, or mEPSCs) recorded in the presence of glia (Fig. 2G). To deter-

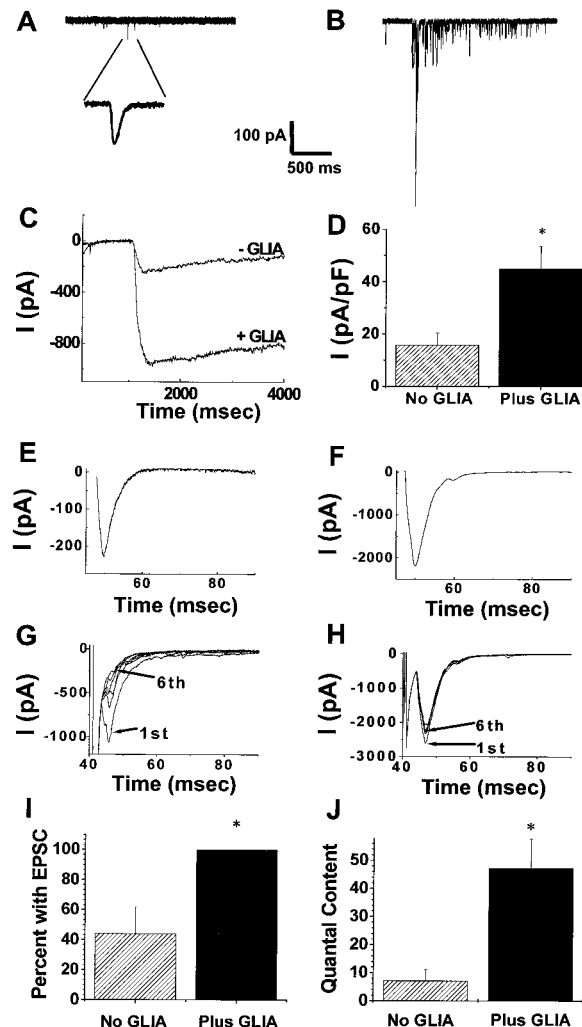


Fig. 1. Glial astrocytes (glia) enhance synaptic efficacy by both presynaptic and postsynaptic mechanisms. (A and B) In the absence of glia, only a low frequency of small spontaneous synaptic currents is observed (A), whereas in the presence of glia large spontaneous synaptic currents are frequently observed (B). All synaptic currents were CNQX-sensitive (10). (C) Application of 50-ms pulses of 100 μM L-glutamate to RGC cell bodies at a holding potential of -70 mV results in sustained inward currents. (D) Current densities of RGCs cultured in the absence or presence of glia. Whole-cell currents: RGCs without glia, 15.7 ± 4.7 pA/pF; RGCs with glia, 45 ± 8.6 pA/pF ($P = 0.015$, Student's *t* test). (E and F) Autaptic EPSCs from RGCs cultured in the absence (E) or presence (F) of glia. (G and H) Higher synaptic failure rates are seen in RGCs without glia (G) than in RGCs with glia (H). (I) Without glia, 44 ± 18% autaptic neurons have detectable EPSCs, whereas 100% have EPSCs in the presence of glia (Mann-Whitney *U* test, $P < 0.05$). (J) Quantal content of RGCs cultured in the absence of glia is 7 ± 4 compared with 47 ± 10 for RGCs cultured with glia (including failures, $P = 0.004$). Quantal content was determined with the direct method.

Stanford University School of Medicine, Department of Neurobiology, Fairchild Science Building, Stanford, CA 94305-5125, USA.

*To whom correspondence should be addressed at Stanford University School of Medicine, Department of Neurobiology, Fairchild Science Building, Stanford, CA 94305-5125, USA. E-mail: emu@stanford.edu

REPORTS

mine whether astrocytes also enhanced presynaptic function, we measured quantal content (QC) of evoked responses in autaptic neurons cultured with a feeding layer of astrocytes (Fig. 1, E and F) (11, 12), thus allowing us to measure presynaptic differences independently of differences in postsynaptic responsiveness. Glia increased QC by sevenfold (Fig. 1J). In addition, RGCs cultured without glia produced EPSCs only half as often as RGCs cultured with glia (Fig. 1I), and the EPSCs detected without glia had

higher depression rates (Fig. 1, G and H). These findings indicate that glia enhance synaptic efficacy by both a postsynaptic and a presynaptic mechanism.

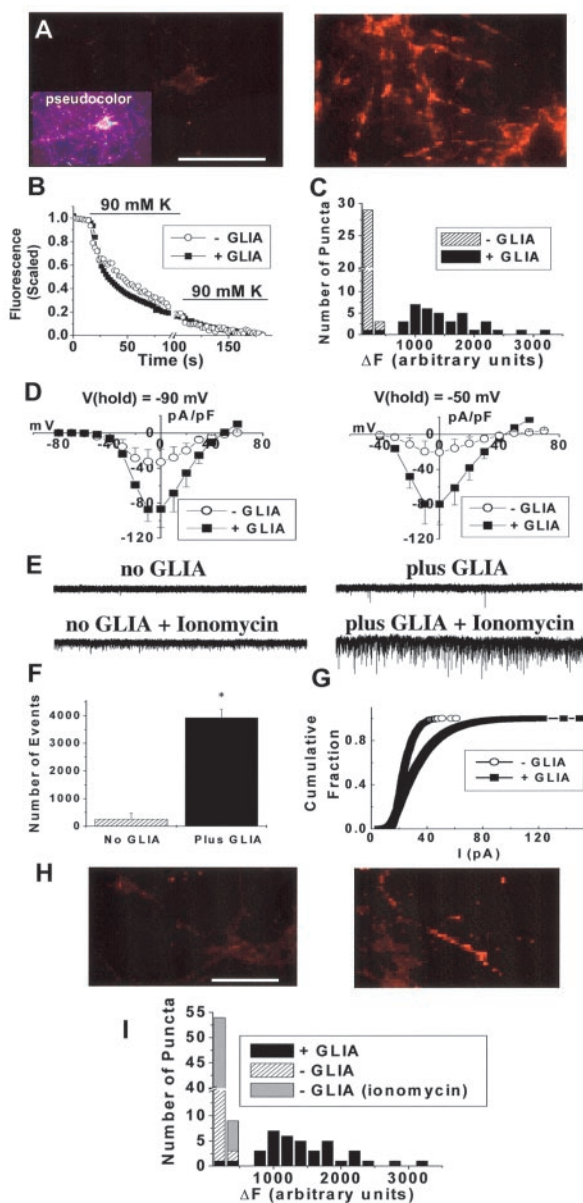
To directly measure presynaptic function without using postsynaptic responsiveness as an indicator, we next examined the ability of RGCs to take up the fluorescent stryryl dye FM1-43 into synaptic vesicles during activity (13–16). Despite a prolonged depolarization, RGCs that had been cultured in the absence of glia took up little FM1-43 compared with

RGCs that had been cultured with glia (Fig. 2A). In both cases, FM1-43 was observed in synaptic punctalike spots along dendrites and somas (Fig. 2A), and these puncta destained with similar kinetics (Fig. 2B). However, glia significantly increased the fluorescence difference ΔF , measured from FM1-43–loaded puncta before and after destaining, by about sevenfold (Fig. 2C). These findings indicate that glia strongly enhance presynaptic function (17).

To determine whether glia enhance presynaptic efficacy by increasing calcium influx, and thereby triggering synaptic vesicle release (18), we next compared the density of voltage-dependent calcium currents in RGCs cultured in the presence and absence of glia by measuring whole-cell calcium-current densities at two different holding potentials (–90 and –50 mV). At both holding potentials, glia increased calcium current density by about two- to threefold (Fig. 2D), suggesting that an increased presynaptic calcium influx might account for the glial enhancement of presynaptic function. To test this possibility directly, we bypassed the endogenous presynaptic voltage-gated calcium channels in RGCs by using the calcium ionophore ionomycin to produce a large presynaptic calcium influx (19, 20). The number of ionomycin-induced mEPSCs recorded was still 10-fold greater in RGCs cultured with glia than without (Fig. 2, E and F). Comparable results were obtained when 500 mM sucrose or 0.3 nM α -latrotoxin were used to trigger vesicular release rather than ionomycin (10). Similarly, when we used ionomycin to load and unload presynaptic terminals with FM1-43, vesicular recycling was still greater in RGCs cultured with glia (Fig. 2H). Notably, the ΔF values measured with ionomycin in RGCs in the absence of glia were indistinguishable from the values measured with high- K^+ stimulation of these neurons (Fig. 2I). These data indicate that glia do not increase presynaptic function solely by increasing presynaptic calcium influx; rather, glia increase the total number of vesicles released.

Given that calcium influx is not sufficient to explain the glial increase in synaptic efficacy, we next examined presynaptic proteins such as the putative calcium sensor synaptotagmin (21). To determine if glia affect synaptic protein levels, we performed immunoblots on extracts of RGCs cultured with or without a feeding layer of astrocytes (22). These analyses show that glia do not appreciably alter the levels of several major presynaptic vesicular proteins including synaptotagmin and synaptophysin (Fig. 3A), as well as SV2 (10). To determine if glia affect the localization of these proteins, we immunostained RGCs that had been cultured with or without astrocytes (23). In the absence of glia, only a diffuse, nonpunctate pattern of

Fig. 2. Glial astrocytes (glia) increase the total number of synaptic vesicles released. (A to C) Labeling of synaptic puncta with FM1-43 in high K^+ . In RGCs cultured in the absence of glia (A, left), FM1-43 weakly labeled puncta; pseudocolor inset shows weakly labeled areas along neurites. In RGCs cultured with glia (A, right), FM1-43 strongly labeled many puncta. (B) Normalized data indicate that puncta destain in the presence or absence of glia with similar time courses. (C) Comparison of the difference in fluorescence intensity (ΔF) between fully stained and fully destained puncta in cells cultured with or without glia. RGCs with glia take up seven times more FM1-43: without glia, mean $\Delta F = 216 \pm 9$; with glia, mean $\Delta F = 1429 \pm 100$ for RGCs [arbitrary fluorescence units, Kruskal-Wallis analysis of variance (ANOVA), $P < 0.001$]. Bar, 50 μm . (D) RGCs cultured with glia display a two- to threefold increase in Ca^{2+} current density at a holding potential of –90 mV (left). Peak current: –33.4 pA/pF without glia, –86.7 pA/pF with glia. RGCs cultured with glia display a nearly threefold increase in Ca^{2+} current density at a holding potential of –50 mV (right). Peak currents: –20.7 pA/pF without glia, –87.1 pA/pF with glia. (E) Ionomycin (5 μM) in the presence of TTX (1 μM) and picrotoxin (50 μM) increases the spontaneous rate of miniature synaptic currents (mEPSCs) in RGCs grown both in the absence (left) and presence (right) of glia. (F) Comparison of the number of mEPSCs detected after treatment with ionomycin indicates that RGCs cultured in the presence of glia have more vesicles available for release. Number of mEPSCs: RGC with glia, 3928 ± 307 events/min; RGCs without glia, 250 ± 217 events/min (ANOVA, $P = 0.0006$). (G) Cumulative amplitude histogram of mEPSC recorded in RGCs in the presence and absence of glia. Mean mEPSC amplitude: with glia, 33 ± 4 pA; without glia, 21 ± 2 pA ($P < 0.05$, Student's t test). Maximum mEPSC amplitude: with glia, 151 pA; without glia, 60 pA. (H and I) Amount of presynaptic vesicle turnover caused by calcium influx with ionomycin treatment visualized with FM1-43. In RGCs cultured without glia, little labeling of presynaptic puncta occurs (H, left) compared with RGCs cultured with glia (H, right). (I) There is no difference between the ΔF values for puncta loaded with ionomycin or 90 mM K^+ in RGCs without glia (ANOVA, $P > 0.5$). Bar, 50 μm .



REPORTS

presynaptic protein immunoreactivity was observed when the cultures were stained with specific antibodies for synaptotagmin (Fig. 3B, left), synaptophysin, or SV2 (10). Only occasional small immunoreactive puncta were observed. In contrast, in the presence of glia, nearly all RGCs displayed numerous large, brightly immunoreactive puncta along their somas and dendrites (Fig. 3B, right). This analysis revealed that, although the absolute levels of synaptic proteins are unchanged, glia have a pronounced effect on the localization of these proteins, promoting their aggregation into synaptic puncta.

To confirm that the large immunoreactive puncta correspond to synapses, we examined whether these puncta that stained brightly with antibodies to presynaptic proteins such as synaptotagmin colocalized with postsynaptic antigens. As shown in Fig. 3, B to D, puncta of presynaptic synaptotagmin were almost always colocalized with puncta of postsynaptic PSD-95 immunoreactivity in the presence of glia. In contrast, few puncta of postsynaptic PSD-95 or GluR2/3 formed in the absence of glia, and there was little colocalization with the few presynaptic puncta that formed. These data show that presynaptic and postsynaptic markers colocalize in puncta that are structural counterparts of synapses in the presence of glia, but rarely in their absence. The glial-dependent clustering and colocalization of synaptic markers was also observed when RGCs were cocultured with their highly purified target neurons from the superior colliculus (24), indicating that the inability of RGCs to form synapses without glia cannot be accounted for by the absence of their normal target neurons [see supplemental data (25)].

To determine if these puncta correspond to functional synapses, we counted synaptic puncta on autaptic neurons using immunostaining (Fig. 3E). Glia increased the number of GluR2/3-positive synaptic puncta by sixfold (Fig. 3F). The average number of immunoreactive puncta that formed on RGCs in the presence and absence of glia was 35 ± 4 and 6 ± 1 , respectively. By comparison, the average number of quanta released in response to a strong stimulation in autaptic neurons cultured in the presence and absence of glia was 47 ± 10 and 7 ± 4 , respectively. The similarity of these values suggests that the immunoreactive puncta that form in the presence of glia correspond to functional synapses. They also indicate that few synapses form between RGCs in the absence of glia and that glia increase the total number of synapses per RGC by six- to sevenfold. The few synapses that do form in the absence of glia are functionally immature, as indicated by their high failure rates and low uptake of FM1-43. Although functional synaptic activity has been reported within minutes of two

excitable cells coming into contact, a mature ultrastructural appearance takes days to develop (26–28). To determine the effect of glia on the ultrastructural characteristics of synapses, we performed electron microscopy (EM) (29, 30). RGC neurons were cultured for 14 days in the presence or absence of glial feeding layers, and then fixed and processed for EM (Fig. 4, A and B). In both cases, synapses were present and displayed the normal ultrastructural characteristics of asymmetric synapses formed by RGCs in vivo (31, 32). RGCs cultured in the presence of astrocyte-conditioned medium, however, had sevenfold more synapses than RGCs cultured in the absence of glia (Fig. 4C). Both the numbers of total vesicles and docked vesicles per synapse were unaffected by glia (Fig. 4D). These data demonstrate that glia significantly increase the average number of synapses per cultured neuron.

To determine whether astrocytes increase synaptic stability, we tested whether the glial effect was reversible. We allowed large numbers of synapses to form by culturing autaptic RGCs with astrocyte-conditioned medium for 5 days, then removed the glia and cultured the RGCs for another 6 days. We found a significant reduction in both the QC and number of synaptic puncta after removal of glia (33). The QC was 47 ± 12 before removal of glia and 14 ± 8 after removal of glia ($P < 0.05$). Postsynaptic GluR2/3 puncta that colocalized with presynaptic SV2 immunoreactivity on autaptic neurons were counted blind. The number of synaptic puncta was 41 ± 4 before removal of glia and 13 ± 1 after removal of glia ($P < 0.001$, Mann-Whitney *U* test). This fourfold reduction in the number of synapses upon removal of glia demonstrates that astrocytes significantly increase synaptic stability and are necessary for synapse maintenance.

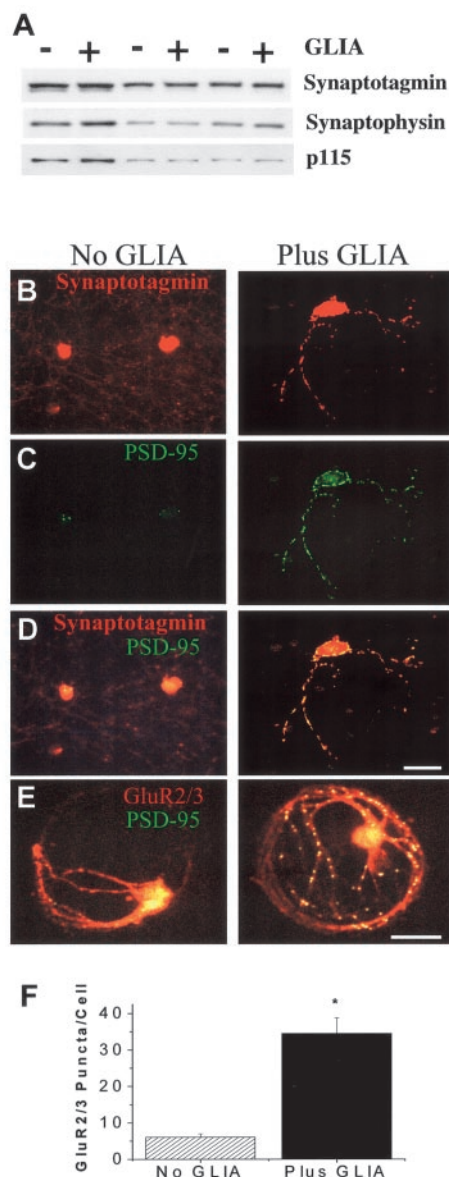
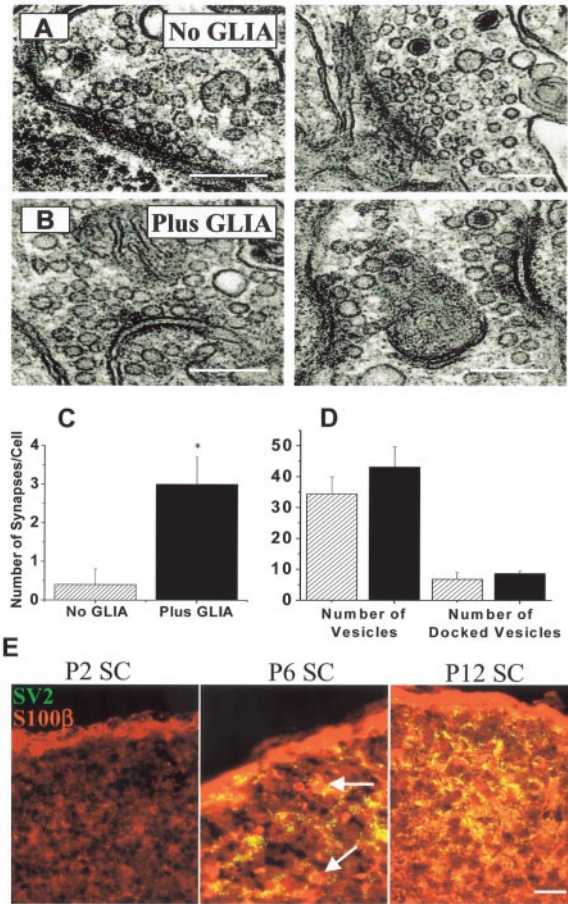


Fig. 3. Glial astrocytes (glia) markedly increase the number of puncta containing both pre- and postsynaptic proteins. **(A)** Immunoblot analysis of extracts of RGCs cultured without glia or with glia indicates no change in total synaptic synaptotagmin and synaptophysin protein levels. p115 is a control for total protein. **(B)** Synaptic protein immunoreactivity in RGCs cultured in the presence and absence of glia. Cultured RGCs were fixed with paraformaldehyde and immunostained with antibodies against pre- and postsynaptic markers. Staining of RGCs with an antibody against the presynaptic marker synaptotagmin shows that in the absence of glia presynaptic markers are diffuse (left), whereas in the presence of glia presynaptic markers are discretely clustered (right). **(C)** Staining of RGCs with an antibody to the postsynaptic marker PSD-95 reveals that in the absence of glia there are relatively few PSD-95 puncta, whereas in the presence of glia numerous puncta are apparent. **(D)** In the absence of glia there is little overlap between pre- and postsynaptic markers, whereas in the presence of glia there is a high degree of overlap. Bar, 50 μ m. **(E)** Double labeling of autaptic neurons indicates that fewer synaptic puncta are present in the absence of glia than in the presence of glia. Bar, 50 μ m. **(F)** About six times as many synaptic puncta are present in RGCs cultured in the presence of glia as in the absence of glia: with glia, 34.5 ± 4.3 GluR2/3 puncta per cell; without glia, 6.1 ± 0.9 GluR2/3 puncta per cell.

REPORTS

Fig. 4. Glial astrocytes (glia) increase the number of synapses per neuron. (A and B) Electron micrographs of synapses between RGC neurons cultured in the absence of glia (A, left and right) and presence of glia (B, left and right). No difference is apparent in synaptic ultrastructure. Bar, 200 nm. (C) The number of synapses detected by EM increased sevenfold in the presence of glia: without glia, 0.4 ± 0.4 ; with glia, 2.8 ± 0.7 per cell body and proximal neurite ($P = 0.013$, Student's *t* test). (D) There are no differences in the total number of vesicles (34 ± 6 without glia, 42 ± 13 with glia) or docked vesicles (6.8 ± 2 without glia, 8.7 ± 0.8 with glia) per synapse. (E) Double labeling of superior colliculus (SC) reveals that synaptic puncta (green) appear around postnatal day 6 (P6), concurrently with the appearance of S100 β -positive astrocytes (red, arrows). Bar, 50 μ m.



These findings raise the question of whether glia also regulate synapse number in vivo. RGC axons reach their targets in the superior colliculus (SC) around embryonic day 16, yet form few synapses, as assessed by both ultrastructural and physiological studies, until around the end of the first postnatal week, as is true in most brain regions (31, 32). To determine whether there is a correspondence between the appearance of synapses and astrocyte development, we immunostained cryosections of the SC at various times during development. The appearance of SV2-positive synaptic puncta in the SC corresponds closely to the appearance and proliferation of S100 β -positive astrocytes at the end of the first postnatal week (Fig. 4E). Taken together with our culture findings, the late appearance of synapses, only after glial generation, strongly suggests that astrocytes trigger the increase in synapse number within the CNS.

In summary, these results show that the total number of synapses on a neuron is not an intrinsic property of that neuron, but can be profoundly regulated by extrinsic signals. In the absence of glia, neurons in culture have only a limited ability to form synapses. Astrocytes greatly increase the number of structurally mature, functional

synapses and are necessary to maintain synaptic stability. These findings have implications for the possible roles of glia in vivo. They suggest that during normal embryonic development, initially formed synapses may be immature and highly plastic, with the postnatal appearance of astrocytes serving to increase synapse number and lock synaptic circuitry in place. In addition, glia may play important and unexpected roles in adult neural plasticity underlying learning and memory. Finally, our results raise the question of whether the gliosis produced by brain injury increases synapse number, potentially leading to epilepsy and excitotoxic neurodegenerative changes.

References and Notes

1. R. Ventura, K. M. Harris, *J. Neurosci.* **19**, 6897 (1999).
2. D. E. Bergles, C. E. Jahr, *J. Neurosci.* **18**, 7709 (1998).
3. A. Araque, V. Parpura, R. P. Sanzgiri, P. G. Haydon, *Trends Neurosci.* **22**, 208 (1999).
4. B. A. Barres *et al.*, *Neuron* **1**, 791 (1988).
5. Purification and culture of RGCs. Step-by-step protocols for all procedures are available on request to barres@stanford.edu. RGCs were purified by sequential immunopanning to greater than 99.5% purity from P6 Sprague-Dawley rats (Simonsen Labs, Gilroy, CA), as described (4). About 15,000 RGCs were cultured per well in 24-well plates (Falcon) on glass (Assistant) or Aclar 22C (Allied Signal) cover slips coated with poly-D-lysine (10 μ g/ml) followed by meroisin (2 μ g/ml) or laminin (2 μ g/ml). RGCs were cultured in 600 μ l of serum-free medium, modified from Bottenstein and Sato

(34), containing Neurobasal (Gibco), bovine serum albumin, selenium, putrescine, triiodo-L-thyronine, transferrin, progesterone, pyruvate (1 mM), glutamine (2 mM), ciliary neurotrophic factor (CNTF) (10 ng/ml), brain-derived neurotrophic factor (BDNF) (50 ng/ml), insulin (5 μ g/ml), and forskolin (10 μ M). Recombinant human BDNF and CNTF were provided by Regeneron Pharmaceuticals. Tetrodotoxin (TTX) and picrotoxin were from RBI. Antibodies were obtained as follows: Anti-synaptophysin (Sigma), anti-GluR2/3 (Upstate Biotech), and anti-PSD-95 (Chemicon). An antibody to synaptotagmin was generated by immunization of a rabbit with a peptide corresponding to the NH₂-terminal luminal portion of synaptotagmin (22). All other reagents were obtained from Sigma.

6. F. W. Pfrieger, B. A. Barres, *Science* **277**, 1684 (1997).
7. K. Christopherson, C. Harrington, S. Venkatapathy, B. A. Barres, data not shown.
8. Preparation of astrocytes. Collicular glia were prepared as described (23). Briefly, p1-2 SCs were digested with trypsin and plated in tissue culture flasks (Falcon) in a medium that does not allow neurons to survive [Dulbecco's minimum essential medium, fetal bovine serum (10%), penicillin (100 U/ml), streptomycin (100 mg/ml), glutamine (2 mM) and Na-pyruvate (1 mM)]. After 4 days, nonadherent cells were shaken off flasks and remaining cells were removed enzymatically and cultured in contact with RGCs unless otherwise stated.
9. Electrophysiology. Membrane currents were recorded by whole-cell patch clamping at room temperature (18° to 22°C) at a holding potential of -70 mV unless otherwise specified. Patch pipettes (3 to 10 megohm) were pulled from borosilicate capillary glass (WPI). For recordings of synaptic currents, the bath solution contained (in mM) 120 NaCl, 3 CaCl₂, 2 MgCl₂, 5 KCl, and 10 HEPES (pH 7.3). The internal pipet solution contained (in mM) 100 K-gluconate, 10 KCl, 10 EGTA (Ca²⁺-buffered to 10⁻⁶), and 10 HEPES (pH 7.3). For recordings of autaptic currents, the internal pipet solution contained (in mM) 122.5 K-gluconate, 8 NaCl, 10 HEPES, 0.2 EGTA, 2 Mg-ATP, 0.3 Na-GTP, 20 K₂-creatine phosphate, and phosphocreatine kinase (50 U/ml). For recordings of calcium currents, the bath solution contained 5 mM BaCl₂, 160 mM tetraethylammonium-Cl, 10 mM HEPES, and 1 μ M TTX. The internal solution contained (in mM) 108 CsMeSO₃, 4.5 MgCl₂, 9 EGTA, 24 HEPES, 4 Na-ATP, and 0.3 Mg-GTP. All data were analyzed with Sigma Stat (SPSS), Origin (Microcal Software), or Mini Analysis Program (Synaptosoft). All tests were Student *t* tests, unless otherwise stated.
10. E. M. Ullian, S. K. Saperstein, K. Christopherson, B. A. Barres, data not shown.
11. B. Katz, R. Miledi, *Proc. R. Soc. London Ser. B* **205**, 369 (1979).
12. J. M. Bekkers, C. F. Stevens, *Proc. Natl. Acad. Sci. U.S.A.* **88**, 7834 (1991).
13. W. J. Betz, F. Mao, G. S. Bewick, *J. Neurosci.* **12**, 363 (1992).
14. W. J. Betz, G. S. Bewick, *Science* **255**, 200 (1992).
15. T. A. Ryan *et al.*, *Neuron* **11**, 713 (1993).
16. Imaging. Cover slips were mounted in a rapid-switching perfusion chamber. Cultures were perfused at room temperature in a saline solution consisting of (in mM) 120 NaCl, 2.5 KCl, 2 CaCl₂, 2 MgCl₂, 25 HEPES (pH 7.4), 10 μ M CNQX (6-cyano-7-nitroquinoxaline-2,3-dione), and 50 μ M APV (D,L-2-amino-5-phosphonopentanoic acid). Synaptic terminals were loaded in the presence of FM1-43 (15 μ M) and 90 mM KCl. After loading, a field containing labeled puncta was chosen. A 4 pixel by 4 pixel area around the center of mass of each of these puncta was imaged with a cooled charge-coupled device camera through a 60 by 1.3 numerical aperture objective mounted on a Nikon diaphot inverted microscope and Metamorph imaging software (Universal Imaging). The FM1-43 was unloaded with 90-s stimulation with 90 mM KCl in FM1-43-free perfusion solution.
17. C. F. Stevens, J. F. Wesseling, *Neuron* **21**, 415 (1998).
18. R. S. Zucker, *Neuron* **17**, 1049 (1996).

Backward Spreading of Memory-Retrieval Signal in the Primate Temporal Cortex

Yuji Naya,^{1*} Masatoshi Yoshida,^{2*} Yasushi Miyashita^{1,2,3,†}

Bidirectional signaling between neocortex and limbic cortex has been hypothesized to contribute to the retrieval of long-term memory. We tested this hypothesis by comparing the time courses of perceptual and memory-retrieval signals in two neighboring areas in temporal cortex, area TE (TE) and perirhinal cortex (PRh), while monkeys were performing a visual pair-association task. Perceptual signal reached TE before PRh, confirming its forward propagation. In contrast, memory-retrieval signal appeared earlier in PRh, and TE neurons were then gradually recruited to represent the sought target. A reasonable interpretation of this finding is that the rich backward fiber projections from PRh to TE may underlie the activation of TE neurons that represent a visual object retrieved from long-term memory.

Encoding and retrieval of declarative memory depends on the integrity and interaction between the neocortex and the medial temporal lobe system (1, 2). The inferior temporal (IT) cortex, which serves as the storehouse of visual long-term memory (3–10), consists of two cytoarchitecturally distinct but mutually interconnected areas (11, 12): area TE (TE) and the perirhinal cortex (PRh). TE is

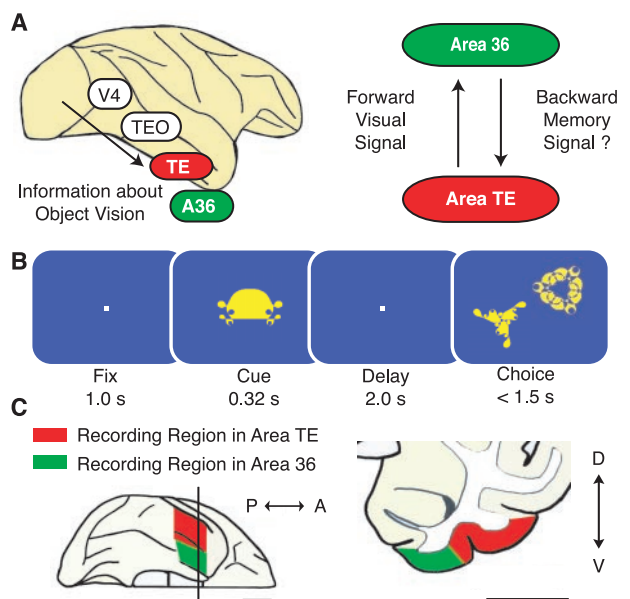
located at the final stage of the ventral visual pathway (Fig. 1A) (13, 14), whereas PRh is a limbic polymodal association area (1, 2). Forward flow of visual information from TE to area 36 (A36), an immediate adjoining region in PRh, is thought to serve the memory-encoding process (5, 6, 15, 16). Recently, we found that memory neurons are more abundant in PRh (16), and that a neurotrophin, BDNF (brain-derived neurotrophic factor), was selectively induced in PRh during memory formation (17), further supporting the hypothesis of memory storage by neural circuit reorganization. However, the function of the rich backward projection from A36 to TE has not been examined. On the basis of previous observations that IT neurons are dynamically activated by the necessity for memory recall in monkeys (18–20), we hy-

¹Laboratory of Cognitive Neuroscience, National Institute for Physiological Sciences, Okazaki, Aichi 444-8585, Japan. ²Mind Articulation Project, International Cooperative Research Project (ICORP), Japan Science and Technology Corporation, Yushima, Tokyo 113-0034, Japan. ³University of Tokyo School of Medicine, Hongo, Tokyo 113-0033, Japan.

*These authors contributed equally to this report.
 †To whom correspondence should be addressed. E-mail: yasushi_miyashita@m.u-tokyo.ac.jp

19. M. Capogna, B. H. Gähwiler, S. M. Thompson, *J. Neurophysiol.* **76**, 3149 (1996).
20. G. Lonart *et al.*, *Neuron* **21**, 1141 (1998).
21. M. Geppert *et al.*, *Cell* **79**, 717 (1994).
22. Western blot analysis. RGC cell lysates were prepared by extraction with 2% SDS. Proteins were resolved by SDS-polyacrylamide gel electrophoresis and transferred onto polyvinylidene difluoride (Millipore). Membranes were incubated in blocking buffer [phosphate-buffered saline (PBS) containing 0.1% Tween-20 and 5% nonfat milk] for 30 min at room temperature, followed by incubation for 1 hour in blocking buffer containing either affinity-purified rabbit antibodies to synaptotagmin luminal domain (1.0 μg/ml), mouse anti-synaptophysin (1:1000; Sigma), or mouse anti-p115 (1:2000) (provided by M. G. Waters, Princeton University). Immunoreactive proteins were detected with horseradish peroxidase (HRP)-conjugated anti-rabbit or anti-mouse immunoglobulin G (1:40,000; Jackson ImmunoResearch) and visualized with a chemiluminescent substrate for HRP (SuperSignal West Pico, Pierce Chemicals).
23. Immunocytochemistry. RGC cultures were fixed in 4% paraformaldehyde in PBS or phosphate buffer (pH 7.4) for 5 min at room temperature and washed in PBS containing 0.3% Triton X-100. Primary antibodies were applied at various concentrations overnight in staining buffer [0.5% bovine serum albumin, 0.5% Triton X-100, 30 mM NaPO₄ (pH 7.4), 750 mM NaCl, 5% normal goat serum, and 0.4% NaN₃]. Secondary antibodies, goat anti-mouse and anti-rabbit Alexa 488 and Alexa 594 conjugates (Molecular Probes), were used at a dilution of 1:200 for 1 hour at room temperature. All washes were done with PBS containing 0.1% Triton X-100.
24. Target SC neurons were purified as described (6). Briefly, SC neurons were dissociated in papain, and microglia, macrophages, and oligodendrocytes were removed by panning with the Gr1phonia Symplicifolia lectin 1 (Vector Labs) and the O4 antibody. Neurons were then selected with an ASCS4 monoclonal antibody (DSHB).
25. Supplementary data are available on Science Online at www.sciencemag.org/cgi/content/full/291/5504/657/DC1.
26. P. G. Haydon, P. Drapeau, *Trends Neurosci.* **18**, 196 (1995).
27. S. E. Ahmari, J. Buchanan, S. J. Smith, *Nature Neurosci.* **3**, 445 (2000).
28. H. V. Friedman *et al.*, *Neuron* **27**, 57 (2000).
29. T. Schikorski, C. F. Stevens, *J. Neurosci.* **17**, 5858 (1997).
30. Electron microscopy. Cells were prepared for EM as described (6). Briefly, cells were washed in 0.1 M phosphate buffer (pH 7.2), then fixed for 30 min in 2% glutaraldehyde buffered with 0.1 M sodium phosphate (pH 7.2) at 4°C. After rinsing with buffer, specimens were stained en bloc with 2% aqueous uranyl acetate for 15 min, dehydrated in ethanol, and embedded in poly/bed812 for 24 hours. Fifty-nanometer sections were poststained with uranyl acetate and lead citrate and viewed with a Philips Electronic Instruments CM-12 transmission electron microscope.
31. R. D. Lund, J. S. Lund, *Brain Res.* **42**, 1 (1972).
32. S. S. Warton, R. McCart, *Synapse* **3**, 136 (1989).
33. Reversal experiments. RGCs were cultured with glia for 5 days, after which the glia were removed and the media exchanged for fresh media. Control RGCs were recorded after 5 days of coculture with glia and exchange of media for astrocyte-conditioned media.
34. J. E. Bottenstein, G. H. Sato, *J. Neurosci.* **76**, 514 (1979).
35. We thank E. Kavalali for advice on FM1-43 experiments, J. Waters and P. De Koninck for critically reading a draft of the manuscript, and M. Hernandez for technical assistance. Supported by a McKnight Investigator Award (B.A.B.), a Kirsch Investigator Award from the Steven and Michele Kirsch Foundation (B.A.B.), and NIH grant NS10784 (E.M.U.).

Fig. 1. (A) Left panel: Lateral view of a macaque brain. TE is located at the final processing stage of the ventral visual pathway. A36 is thought to be a part of the medial temporal lobe memory system. V4, visual area 4; TEO, area TEO. Right panel: Role of the backward connection from A36 to TE. A36 receives forward visual signal from TE. (B) Sequence of events in a trial of the PA task. Fixation points and cue stimuli were presented at the center of a video monitor. Choice stimuli were presented randomly in two of four positions on the video monitor. (C) Location of recording sites in TE (red) and A36 (green). Left panel: Ventral view of a monkey brain (anterior at the right). Right panel: A part of the coronal cross section (dorsal at the top) indicated by a horizontal line on the ventral view. Scale bars, 10 mm.



18 September 2000; accepted 26 December 2000

This copy is for your personal, non-commercial use only.

If you wish to distribute this article to others, you can order high-quality copies for your colleagues, clients, or customers by [clicking here](#).

Permission to republish or repurpose articles or portions of articles can be obtained by following the guidelines [here](#).

The following resources related to this article are available online at www.sciencemag.org (this information is current as of February 5, 2015):

Updated information and services, including high-resolution figures, can be found in the online version of this article at:

<http://www.sciencemag.org/content/291/5504/657.full.html>

Supporting Online Material can be found at:

<http://www.sciencemag.org/content/suppl/2001/01/26/291.5504.657.DC1.html>

A list of selected additional articles on the Science Web sites **related to this article** can be found at:

<http://www.sciencemag.org/content/291/5504/657.full.html#related>

This article **cites 20 articles**, 9 of which can be accessed free:

<http://www.sciencemag.org/content/291/5504/657.full.html#ref-list-1>

This article has been **cited by** 427 article(s) on the ISI Web of Science

This article has been **cited by** 100 articles hosted by HighWire Press; see:

<http://www.sciencemag.org/content/291/5504/657.full.html#related-urls>